IEEE Photonics Journal
An IEEE Photonics Society Publication

Open Access

Second-Order Nonlocal Effects Mitigation in Brillouin Optical Time-Domain Analysis Sensors by Tracking the Brillouin Frequency Shift Profile of the Fiber

Volume 9, Number 5, October 2017

Juan José Mompó
Haritz Iribas
Javier Urricelqui
Alayn Loayssa, *Member, IEEE*

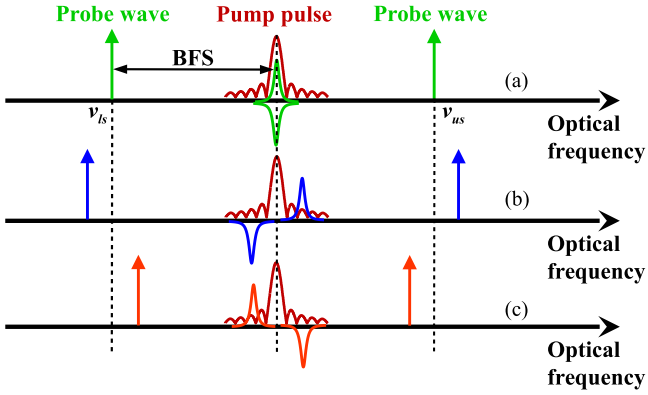

DOI: 10.1109/JPHOT.2017.2748965
1943-0655 © 2017 IEEE

Second-Order Nonlocal Effects Mitigation in Brillouin Optical Time-Domain Analysis Sensors by Tracking the Brillouin Frequency Shift Profile of the Fiber

Juan José Mompó, Haritz Iribas, Javier Urricelqui, and Alayn Loayssa, *Member, IEEE*

Department of Electrical and Electronic Engineering, Universidad Pública de Navarra, Pamplona 31006, Spain

DOI:10.1109/JPHOT.2017.2748965

Manuscript received May 10, 2017; revised August 23, 2017; accepted August 31, 2017. Date of publication September 12, 2017; date of current version September 25, 2017. This work was supported by the Universidad Pública de Navarra, Feder funds and Spanish Ministerio de Economía y Competitividad through the project TEC2013-47264-C2-2-R and TEC2016-76021-C2-1-R. Corresponding author: Alayn Loayssa (e-mail: alayn.loayssa@unavarra.es).

Abstract: We report on an additional limitation that has been found in Brillouin optical time-domain analysis (BOTDA) sensors due to the so-called second-order nonlocal effects (NLE). Second-order NLE appear in BOTDA setups that deploy a double probe waves to compensate the transfer of energy between the pump pulse and the probe wave, and are related to a spectral distortion of the pump pulse that leads to measurement errors and an effective limit on the maximum probe power that can be deployed in the sensor. We theoretically and experimentally demonstrate that the techniques that have been presented so far in the literature to compensate second-order NLE are only effective in the case that the Brillouin frequency shift (BFS) along the sensing fiber is uniform. However, this requirement for uniformity is not realistic in real world scenarios in which a variety of fibers with different BFS and subjected to different environmental conditions are typically deployed. Therefore, we demonstrate a new method to mitigate the effects of BFS variation in the BOTDA setups that compensate second-order NLE. This method is based on introducing an additional wavelength modulation to the probe wave so as to track the mean BFS changes along the sensing fiber link. With this method, we demonstrate a BOTDA setup that, without coding, distributed amplification, or any other form of performance enhancement, achieves a sensing length of 120 km with 3-m spatial resolution and 2-MHz measurement precision. Moreover, the setup demonstrates, to our knowledge, the largest probe power ever injected in a BOTDA sensing link.

Index Terms: Stimulated Brillouin scattering, brillouin optical time-domain analysis (BOTDA), fiber optics sensors, second-order nonlocal effects (NLE).

1. Introduction

Brillouin optical time-domain analysis (BOTDA) sensors have been commonly deployed to ensure the integrity of structures such as oil and gas pipelines or high voltage transmission lines. These, and other applications have a common need for distributed sensors that can monitor large distances. However, the attenuation of the optical fiber ultimately limits the sensing length of BOTDA sensors due to its effect on the counterpropagating pump and probe waves that are deployed in these

systems. The pump pulse attenuates as it propagates along the fiber so that the Brillouin gain experienced by the probe wave at far away locations becomes very small, hence leading to a reduced signal-to-noise ratio (SNR) of the measurement and large measurement errors. This can be compensated to some extent by increasing the pump pulse power, but non-linear effects, particularly modulation instability (MI), typically limit the maximum power to a few hundred milliwatts. Solutions to the problem of pulse attenuation have been proposed using distributed amplification based on Raman as well as Brillouin scattering [1], [2].

As for the probe wave, its attenuation by the fiber leads to a reduced probe power level reaching the receiver, which also translates into a degradation of the measured SNR and the performance of the sensors. Again, the obvious solution to this issue is to increase the probe power level injected in the fiber. However, this improvement mechanism is limited first by the onset of the so called non-local effects (NLE) and, for higher powers, by noise induced by spontaneous Brillouin scattering (SpBS) on the detected probe wave once its power overtakes the Brillouin threshold of the sensing fiber link.

NLE are due to the transfer of energy from the pump pulse to the probe wave, which generates a frequency-dependent pump depletion. This distorts the measured Brillouin interaction spectrum and induces a biasing effect and an error in the Brillouin frequency shift (BFS) determination. This effect limits the maximum probe power to around -14 dBm for 1-MHz maximum tolerable BFS measurement error, assuming typical parameters for long standard single mode fiber links [3]. Solutions to compensate this first-order NLE have been proposed in the form of BOTDA setups that deploy two probe waves, one with higher and the other with lower frequency than the pump, which generate a balanced gain and loss interaction upon the pulsed pump signal [4]. However, in these systems, a second-order NLE comes into play because the Brillouin gain and loss spectra generated by the two probe waves only overlap and compensate perfectly when the frequency difference between pump and probe waves equals the BFS of the fiber. For other frequency differences, during the Brillouin spectrum scan process, the spectra do not overlap and the spectrum of the pump pulse signal is distorted [5]. This effect limits the maximum probe wave power to around -3 dBm, again for typical long-range BOTDA systems.

Several techniques have been implemented in order to counteract the second-order NLE. An smart solution is to modify the conventional frequency sweep used to retrieve the Brillouin spectrum so that the Brillouin gain and loss spectra always overlap over the pulsed signal during the whole scan process. This has been demonstrated by fixing the optical frequency difference of both prove waves during the scanning to twice the BFS of the fiber [6]. An improved version of this system uses four probe waves [7]. Nevertheless, even though this method, in principle, mitigates the problem of second-order NLE, it is still limited by SpBS, so that the maximum probe power is limited for long-range links to around 7 dBm by the Brillouin threshold.

We have recently demonstrated another solution to the problem of second-order NLE that is based on a BOTDA with two probe waves in which the wavelength/frequency of the probe waves is modulated so as to achieve a flat interaction spectra on the pulse that do not distorts its spectrum [8]. This technique has the added advantage that, besides compensating second-order NLE, it also provides the possibility to inject probe powers in the fiber that exceed the Brillouin threshold. This is a side effect of the wavelength modulation of the probe, which is a well-known method to increase the effective Brillouin threshold in a fiber link.

In this paper, we report on an additional limitation that has been found in the previously mentioned BOTDA sensor configurations that try to compensate second-order NLE. We theoretically and experimentally demonstrate that the techniques that have been presented so far to compensate second-order NLE are only effective in case that the BFS along the sensing fiber is uniform. However, this requirement for uniformity is not realistic in real-world field-application scenarios in which a variety of fibers with different BFS and subjected to different environmental conditions are typically deployed. We perform a detail modelling of the effect of non-uniformity of the BFS along the fiber and demonstrate its agreement with experimental measurements. Furthermore, we introduce a new method to compensate second-order NLE that works with any distribution of BFS along the fiber and that is based on dynamically modifying the wavelength of the probe wave to

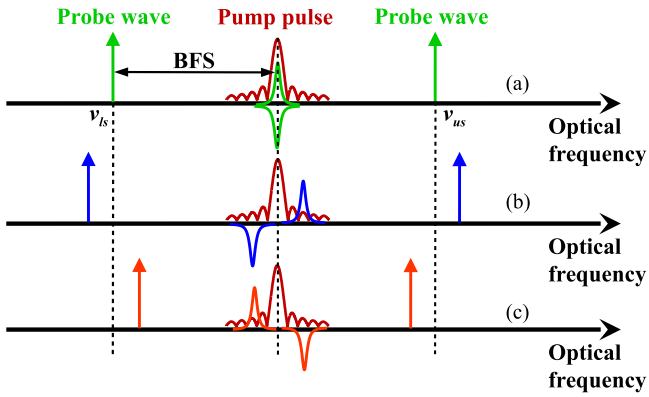

Fig. 1. Brillouin interaction on the pump pulse in BOTDA sensors with double probe wave during the spectral scanning process when the frequency spacing of the probes from the pump (a) equals, (b) is larger, or (c) is smaller than BFS of the sensing fiber.

adapt to the changes in average BFS of each section of the fiber sensing link. We use this method in a 120-km sensing link in which we deploy the highest probe power injected in the fiber that, to the best of our knowledge, has been demonstrated in any BOTDA setup. This provides a good performance for this link without the need to use additional techniques such as pulse coding or distributed amplification of pulses.

2. Second-Order NLE in Non-Uniform BFS Fiber Links

Second-order NLE are due to the spectral distortion of the pump pulse signal when it continuosly interacts with the Brillouin spectra induced by the two probe waves deployed in NLE-compensating BOTDA sensors [5]. As depicted in Fig. 1(a), the use of two probe waves equally spaced from the pulsed pump signal by the BFS of the fiber is enough to solve the problem of first-order NLE, since the Brillouin gain spectrum generated by one of the probe waves upon the pulsed signal is canceled out with the Brillouin loss spectrum induced by the other probe wave. However, during the scanning process used to retrieve the Brillouin spectrum, the frequency spacing of both probe waves from the pump is shifted. As a consequence, the Brillouin spectra generated by both probe waves do not longer overlap over the pulsed signal, inducing an spectral distortion of the pulse, as it is schematically depicted in Fig. 1(b) and (c). The onset of this spectral distortion effectively limits the maximum probe power to around -3 dBm for typical long-range BOTDA systems [5].

In order to solve the limitation set by the described second-order NLE several solutions have been proposed [6], [7]. One solution is to maintaining a constant frequency difference between both probe waves during the scanning process, which should be fixed to twice the BFS of the fiber as depicted in Fig. 2(a) [6]. However, whenever the BFS varies along the fiber, the Brillouin gain and loss spectra generated by the probe waves do not longer overlap giving rise to a non-flat transfer function over the pulsed signal as it can be observed in Fig. 2(b) and (c). Moreover, as it is analyzed below, this issue can not be solved in general by adjusting the probe spacing using the average BFS of a particular portion of the fiber, for instance, to the BFS of the so-called effective length from the probe input end. The Brillouin gain and loss is so large due to the powerful probe wave injected into the fiber that even when the probe wave has been greatly attenuated by the fiber propagation, the interaction between the pump and probe wave can still introduce significant spectral distortion on the pump pulse spectrum [7].

The solution that we proposed to overcome second-order non-local effects is based on the frequency modulation of the optical probe waves [8]. The Brillouin spectral interaction induced on the pulse in this technique is schematically depicted in Fig. 3. As it is shown, the frequency modulation of the optical probe waves broadens the total Brillouin interaction experienced by the

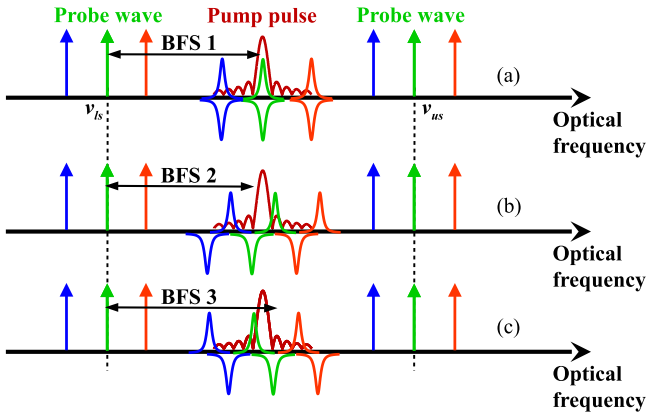

Fig. 2. Brillouin interaction on the pump pulse in BOTDA sensors with two probe waves that maintain constant frequency spacing during the scanning process when the frequency spacing of the pump between the probes (a) equals, (b) is larger, or (c) is smaller than twice the BFS of the sensing fiber. Different colors (red, blue, green) are shown for different frequencies of the probes waves during the spectral scanning process.

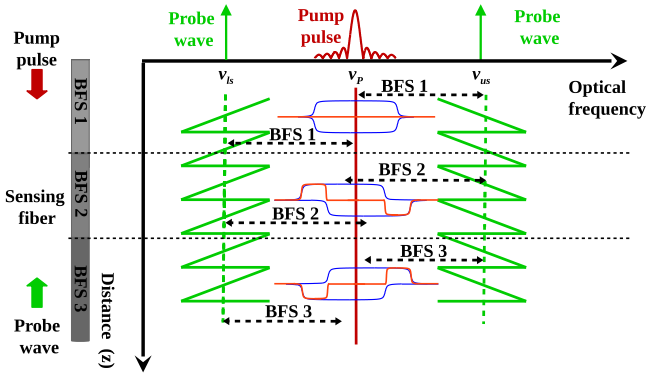

Fig. 3. Brillouin interaction on the pump pulse in BOTDA sensors with frequency modulation of the probe waves when the mean frequency spacing of the probes from the pump (BFS 1) equals, (BFS 2) is smaller, or is larger than the BFS of the sensing fiber (BFS 3).

pulsed signal [8]. Adjusting the average frequency of both probe waves to the BFS of the fiber, both spectra cancel out leading to no distortion of the pulse. However, as in the previous case, if there is a section of the fiber that has a different BFS, both interactions shift and hence, the pulse becomes affected by a non-flat transfer function, as shown in Fig. 3. Notice that the influence of the Brillouin interaction over the pulsed signal is going to be less significant with our method based on frequency-modulated probe waves that the one deploying constant frequency separation between the probes, since the frequency modulation spreads the energy of the interaction into a larger frequency region, thus, reducing the amplitude of the transfer function. However, there is still some distortion of the high frequency components of the pulse that, as it is shown below, limits the maximum probe power that can be deployed in links with BFS variation along the fiber.

In summary, we have qualitatively shown that all techniques available so far to compensate second-order NLE require the fiber to have a fairly uniform BFS along its length. The use of fiber with varying BFS characteristic leads to a residual second-order NLE that may affect the pulsed signal. In order to quantify this effect we can solve the differential equations governing Brillouin interaction between the pump pulse and the probe waves assuming that the intensity of the probe waves along the fiber is not affected by the pump wave interaction [9]. This gives the expression of

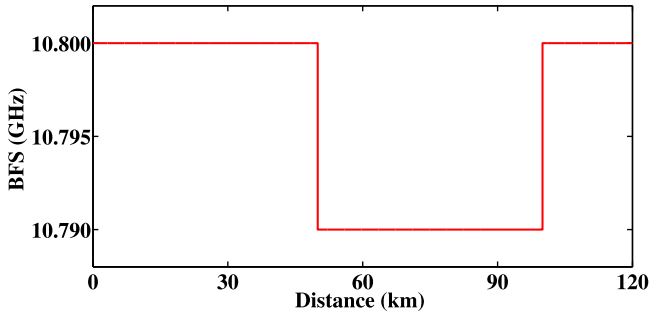

Fig. 4. BFS profile used for simulation.

the pump pulse propagating along the fiber:

$$P_p(z) = P_p(0)exp\left[P_{us}(0)\int_0^z \frac{g_b(\Delta\nu_{us})}{A_{eff}}e^{\alpha z}dz - P_{ls}(0)\int_0^z \frac{g_B(\Delta\nu_{ls})}{A_{eff}}e^{\alpha z}dz\right]e^{-\alpha z} \quad (1)$$

where $P_p(0)$, $P_{us}(0)$ and $P_{ls}(o)$ are the power of the pump wave, and upper and lower frequency probe waves, respectively, at the input of the fiber, α is the fiber attenuation, A_{eff} is the effective area, and g_B is the Brillouin gain or loss spectra at each location, z, that depends on the local frequency detuning $\Delta\nu_{us}$ and $\Delta\nu_{ls}$, respectively, given by:

$$\Delta\nu_{us} = \nu_p + \nu_{us}(z) - BFS(z) \quad (2)$$

$$\Delta\nu_{ls} = \nu_p - \nu_{ls}(z) + BFS(z) \quad (3)$$

where ν_p, ν_{us} and ν_{ls} are the optical frequencies of pump, and upper and lower frequency probe waves, respectively, and BFS is the Brillouin frequency shift in each location of the fiber. The solution in (1) assumes pulses with a duration longer than the acoustic phonon lifetime ($\sim$10 ns).

As an example of the distortion brought by second-order NLE in non-uniform BFS fiber links, we use the model in (1) to calculate the spectral distortion of the pulse in a link with the BFS distribution shown in Fig. 4. The fiber link comprises two consecutive 50-km fiber sections with 10.8 and 10.79 GHz and another fiber section of 20 km with a BFS value, again, of 10.8 GHz. This is quite a realistic scenario in which two types of fibers with slightly different BFS due to fabrication or cabling are deployed in a link.

The total transfer function due to Brillouin interaction experienced by the pulsed signal when injecting different probe power levels in the link is calculated when using either the technique for second-order NLE compensation deploying two probes with constant frequency spacing during the spectral scanning (Fig. 5(a)), or our method with frequency modulation of the probe waves (Fig. 5(b)). Note that the horizontal axis represents the frequency deviation from the central frequency of the pulse spectrum.

In both systems, the peak-to-peak frequency deviation of the probe waves is 300 MHz and the frequency of the probe waves for perfect compensation of second-order NLE is set assuming a BFS value of 10.8 GHz, which is predominant in the fiber, particularly in the first 20-km section at the probe wave input end. The first fact that the calculations in Fig. 5 highlights is that adjusting the probe wave frequencies taking into account just the BFS of a section of the fiber approximately equal to its effective length is not sufficient to get rid of second-order NLE. Indeed, the calculations display significant spectral distortion of the pump pulse spectra even at moderate probe powers. In addition, the calculations in Fig. 5 also highlight that the technique for second-order NLE compensation using frequency modulation of the probe waves is more tolerant to BFS variation than the method using probe waves with constant frequency spacing: at equal power level the amplitude of the spectral distortion is much lower. Up to 10 dB larger probe power can be deployed with the frequency modulation method for same-order distortion. As it was explained before, this advantage is due to the spreading of the interaction upon the pump pulse into a large frequency region brought by the

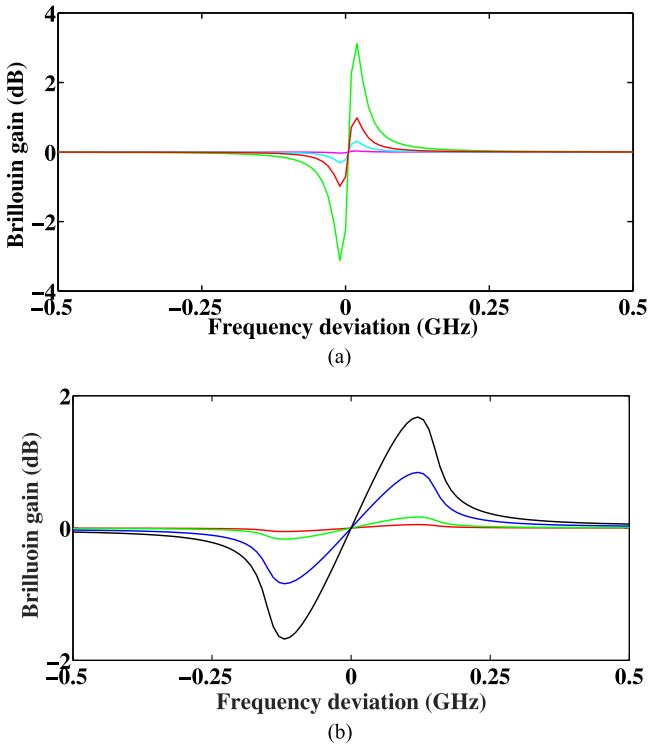

Fig. 5. Brillouin interaction frequency response (a) for the system presented in [6] using a probe power of −15 dBm (magenta), −5 dBm (cyan), 0 dBm (red) and 5 dBm (green) and (b) using the FM technique presented in [8] when the probe levels are 0 dBm (red), 5 dBm (green), 12 dBm (blue) and 15 dBm (black).

frequency modulation of the probe, which reduces the maximum level of distortion experienced by the pulse.

3. Second-Order NLE Mitigation by BFS Tracking

We propose a novel method to solve the limitation on probe wave power imposed by the non-uniformity of the BFS along the fiber in BOTDA setups that compensate second-order NLE. This method is based on dynamically tuning the optical frequency of the probe wave so that it tracks the changes in BFS along the fiber. This is achieved by introducing an additional optical frequency modulation to the probe wave. A schematic of the fundamental of this new technique is depicted in Fig. 6. As it can be observed a frequency shift is added to the probe wave optical frequency modulation. This added frequency shift must be set so that the average frequency of the probe waves matches the average BFS of each section of the fiber. Therefore, the gain and loss spectra induced by both probe waves on the pump pulse frequencies cancels out at each section of the fiber so that the spectral distortion that was analyzed above is avoided.

Notice that the BFS tracking just described does not need to be very precise or very fast. It is necessary just to adapt to changes in the average BFS profile of different sections of the fiber. This profile can be extracted from the measurements that the BOTDA system is continuously performing or even from a previous characterization of the BFS along the fiber using low spatial resolution, as it will be shown in the following sections. The system can work with sharp changes in BFS profile due to the use of different fiber types concatenated as well as with slow variations of the average BFS of the fiber link due to enviromental or cabling effects. Minor deviations of the local BFS in small lengths of fiber are not significant because their contribution to the total integrated gain and loss affecting the pulse is going to be small.

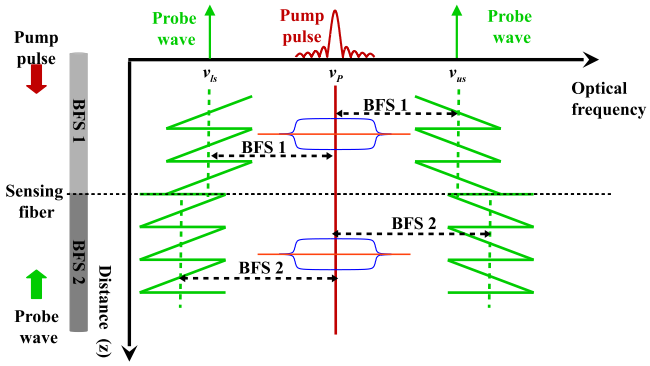

Fig. 6. Schematic of the fundamentals of the technique for compensation of BFS changes along the fiber in a BOTDA setups that uses frequency modulation of the probe wave optical frequency to mitigate second-order NLE. An example scenario in a fiber with two sections having different BFS is depicted. A frequency offset is added to the optical frequency modulation of the probe wave so as to make the central frequency of the probe wave match the BFS at each location.

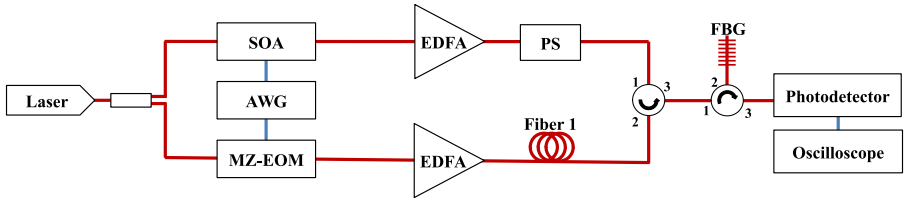

Fig. 7. Experimental setup for the BOTDA sensor based on tracking the BFS with frequency modulation of the probe wave.

4. Experimental Setup

In order to evaluate the potential of the technique, the experimental setup depicted in Fig. 7 was assembled [8]. The output of a distributed feedback (DFB) laser is divided by a coupler into two branches to generate the pump and probe waves. In the upper branch, the output of the coupler is pulsed by a semiconductor optical amplifier (SOA) driven by an electrical pulse from an arbitrary waveform generator (AWG). The pump pulse is boosted to a peak of 19 dBm using an Erbium-doped fiber amplifier (EDFA), and its state of polarization (SOP) is randomized using a polarization scrambler (PS).

In the lower branch, a dual-probe wave is generated using a Mach-Zehnder electro-optical modulator (MZ-EOM) that is biased at the minimum transmission point of its transfer curve to generate a double sideband suppressed-carrier signal. The MZ-EOM is driven by an AWG, which provides a microwave signal with a saw-tooth frequency modulation centered at 10.8 GHz and with a peak-to-peak frequency deviation of 300 MHz. Also, the AWG provides a synchronization between the electrical pulse and the FM modulation of the microwave signals in order for the pump pulses to always interacts with the same instantaneous frequency at the same location of the fiber [8]. The power of the probe waves is amplified in another EDFA before being injected into the sensing fiber in a counter-propagate direction to the pump pulse. Finally, after Brillouin interaction of these waves with the pump pulse, the probe waves are directed to a fiber Bragg grating via a circulator in order to filter out the upper-frequency probe, and the remaining lower-frequency probe is detected by a photo-detector, which is connected to an oscilloscope.

5. Experimental Results

A 120-km length of standard single-mode fiber (ITU G.652) with different BFS sections was deployed in the setup of Fig. 7 in order to analyze the detrimental effect that a non-uniform BFS profile of

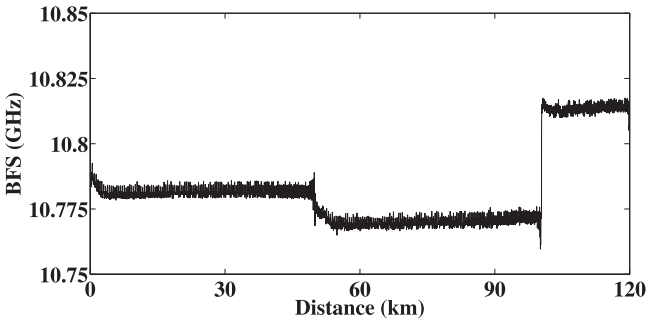

Fig. 8. Measured BFS distribution along the fiber.

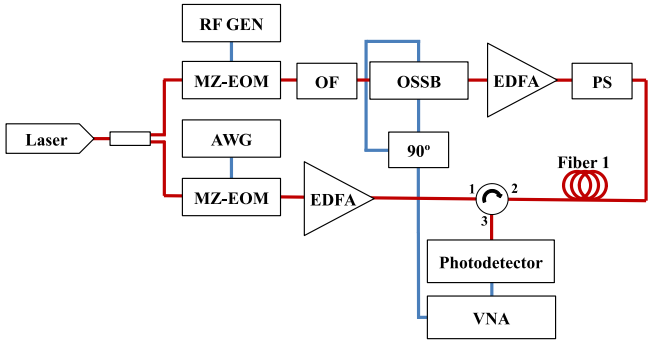

Fig. 9. Experimental setup used in order to characterize the optical frequency response of the Brillouin interaction that the pump wave spectrum experiences.

the sensing fiber has on the compensation of second-order NLE, and also to demonstrate the capabilities of the proposed tracking technique to overcome this impairments. Fig. 8 shows the measured BFS profile of the fiber, where three different fiber spools with a slightly different BFS are clearly distinguishable. The BFS difference between the first two reels (50-km length each) was around 17 MHz, while the deviation between the second and third one (this one with 20-km length) was 46 MHz. This measurements were performed using the setup in Fig. 7 without adding the BFS tracking capability. The probe power was 12 dBm and long duration pulses of 200 ns were used because we were interesting just in the evolution of the average BFS along the fiber. During measurements, the last 20 km of the fiber was kept at constant controlled temperature in a climatic chamber.

We started by characterizing the optical frequency response experienced by the pump wave as a result of its interaction with the probe waves. In order to perform this measurement we devised the experimental setup in Fig. 9, which is a modification of that in Fig. 7. The idea was to deploy the technique for optical transfer function measurement based on the use of optical single-sideband (OSSB) modulation [10]. We modified the upper branch of the setup in Fig. 7 to generate a OSSB signal whose sideband could be tuned in the range of frequencies of the pump pulse. Then, this OSSB signal counter-propagates with the probe waves so as to make the sideband experience the same transfer function that the pump pulse would experience. Finally, the OSSB signal is extracted at the far end of the fiber using a circulator and detected in a microwave bandwidth photodetector, which translates the optical transfer function from the optical to the electrical domain [10]. In addition, a 20-GHz electrical vector network analyzer (VNA) is used to scan the frequency of the OSSB sideband and measure the optical transfer function.

The method to derive the OSSB from the laser in Fig. 9 uses first a MZ-EOM biased at minimum transmission and driven by an RF generator at 10 GHz to generate a double-sideband

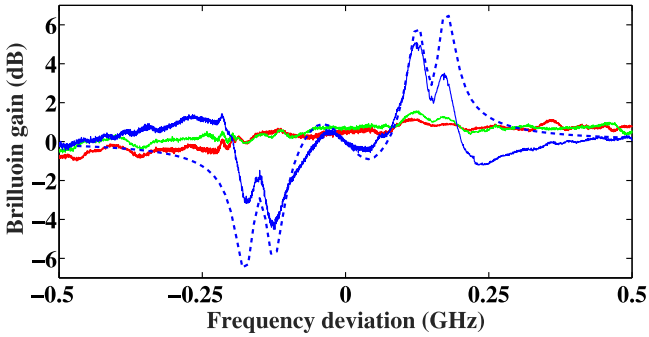

Fig. 10. Measured Brillouin interaction frequency response over the pump pulse when the probe wave is 0 dbm (red), 5 dBm (green) and 15 dBm measurement (solid blue). Also shown (dashed blue) are calculations using (1) and 15-dBm probe wave.

suppressed-carrier signal. The lower-frequency sideband is later removed using and optical filter (OF), which leaves a single spectral component that becomes the optical carrier of the OSSB and is spaced 10-GHz from the pump central frequency. Then this optical carrier is fed to an optical single-sideband modulator (OSSB-EOM), which is based on a MZ-EOM with two RF electrodes driven using a 90 hybrid coupler [11]. The OSSB-EOM is driven by the VNA that scans the side-band frequency, by generating a microwave frequency sweep between 9.5 GHz and 10.5 GHz, and measures the optical transfer function experienced by the pump along the fiber and up to the microwave photodetector.

Fig. 10 depicts the distortion of the frequency transfer function, measured using the OSSB method, for increasing probe power. This is the transfer function that the pump pulse experiences due to its interaction with the probe waves. It can be clearly observed that as the probe power is raised, the distortion of the pump wave increases. Indeed, for probe wave powers of 0 dBm and 5 dBm the pump wave spectral distortion is negligible. However, when the probe power is increased to 15 dBm, the pump wave spectrum experiences a large distortion: the low and high frequencies of the spectrum experience a 4-dB peak loss and gain, respectively. Besides, this last measurement is compared in the figure with the calculations using the model in (1), showing good agreement in shape, despite some small differences attributable to the SpBS generated over the OSSB signal frequencies by the counterpropagating continuous probe waves. Notice that the frequency separation of the gain and loss peaks in Fig. 10 equals the peak-to-peak frequency deviation of the FM modulation introduced to the probe wave. In addition, the frequencies of the two lobes that each peak can be directly related to the difference between the central frequency of the FM modulated probe waves and the BFS of the different sections of the fiber.

The distortion of the optical transfer function experienced by the pump pulse upon interaction with the probe waves translates to a distortion of the temporal shape of the pulses. This is highlighted in Fig. 11, that displays the temporal shape of a 20 ns pulse, measured at the output of the fiber in the setup of Fig. 7, when different probe wave power level are deployed. It can be observed that for probe wave power lower than 12 dBm the pulse shape does not experience nearly any distortion.

However, for 12 dBm probe wave power a ripple of around 11% of the pulse amplitude appears on the top of the pulse. Moreover, for 15 dBm this ripple is increased to a variation of 53% of the amplitude of the pulse and, in addition, the fall edge of the pulse loses its original shape.

Once the detrimental effect on the pump pulse wave that the BFS difference along the sensing fiber had been studied, we experimentally demonstrate the performance of the new BFS tracking technique. For that purpose, the first step is to measure the average BFS profile of the sensing fiber, which was done and displayed in Fig. 8. Then the measured BFS profile is used to compensate the average BFS variation of the fiber, by adding an offset frequency to the probe wave modulation, as it was schematically explained in Fig. 6. Finally, we performed distributed measurements of BFS using 30-ns pump pulses (3-m spatial resolution) and a probe power of 15 dBm. This probe power

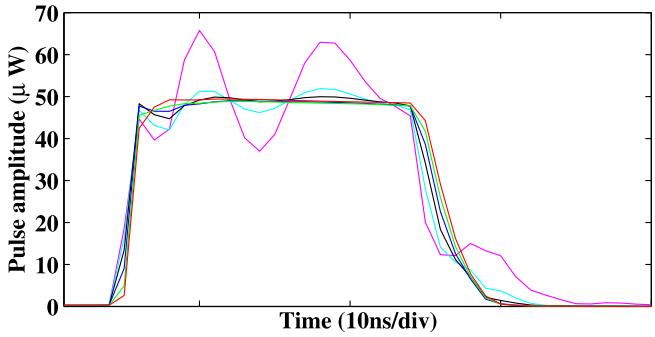

Fig. 11. 20 ns pump pulses at the output of the fiber when the probe wave power is 0 dBm (red), 3 dBm (green), 6 dBm (blue), 9 dBm (black), 12 dBm (cyan) and 15 dBm (magenta).

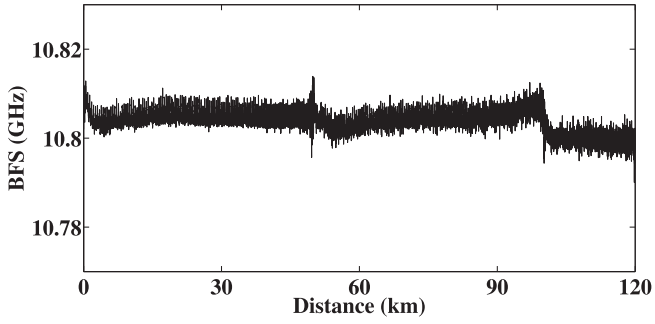

Fig. 12. Measured "virtual" BFS profile along the fiber when the BFS tracking method is deployed.

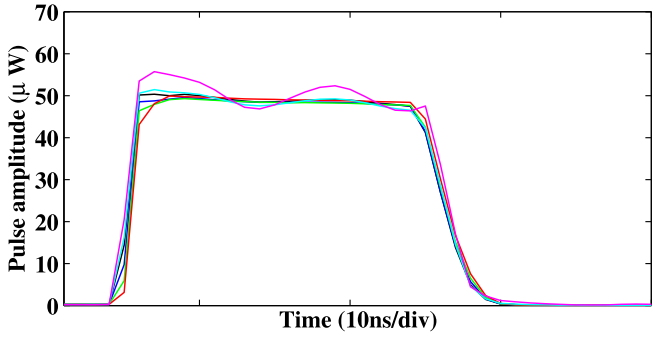

Fig. 13. 20 ns pulses at the output of the fiber when probe wave is 0 dBm (red), 3 dBm (green), 6 dBm (blue), 9 dBm (black), 12 dBm (cyan) and 15 dBm (magenta).

was limited by the Brillouin threshold of the fiber. Fig. 12 shows the measured BFS measurement along the fiber when this BFS tracking is applied. Notice that is a "virtual" BFS since to obtain the real BFS it is necessary to subtract the frequency offset added to the probe wave modulation at each fiber section. The BFS is not completely flat in Fig. 12 because just the last 20 km of the sensing fiber were held inside a climate chamber during measurements. Hence, the first 100 km were exposed to laboratory temperature variations between the initial measurement of the average BFS in Fig. 8 and the measurements with tracking in Fig. 12, which explains that their BFS is slightly offset from 10.8 GHz. Note that in a real system the BFS tracking would be continuously in operation using previous measurement results so the BFS variation would be perfectly compensated.

Fig. 13 depicts the temporal shape of 20 ns pump pulses after crossing the whole fiber and for different probe wave power levels, when BFS tracking is applied. It can be observed, that for a lower

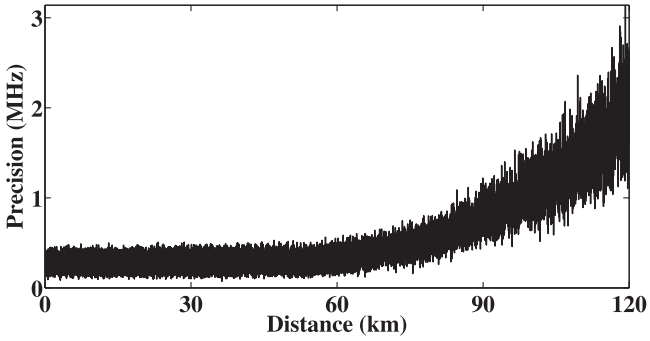

Fig. 14. Precision of the BFS measurement obtained along the fiber.

probe power than 15 dBm there is negligible pulse distortion, while for a probe power of 15 dBm just a small ripple appears and the fall edge of the pulse preserves is original shape. This small distortion, which does not impair measurements, is due to the residual variation of BFS that was observable in Fig. 12. Nevertheless it would be completely suppressed in a system with continuous BFS tracking.

Finally, in order to evaluate the precision of the system, a series of 18 consecutive measurements were performed. Fig. 14 shows the precision along the sensing fiber calculated from the standard deviation of those measurements at each location. An approx. 2-MHz (1σ) precision is obtained at the end of the fiber. All these measurements have been done with 1024 averages of the traces.

6. Conclusion

In this paper, we have introduced the way to obtain the ultimate performance of BOTDA sensors in terms of the probe power that they can deploy. We have identified the factor that was limiting the performance of currently available NLE compensation methods: the inability of those methods to cope with variations of the BFS profiles along the fiber. This is a limitation that really limits real world applications of long-range BOTDA sensors. We have demonstrated that indeed this was the limiting factor by developing a theoretical model for the pump pulse distortion due to the interaction with the probe waves. Furthermore, we have verified this model experimentally.

In addition, we have presented a new technique that makes BOTDA sensors to completely compensate NLE by adding an optical frequency modulation to the probe to track the variations in average BFS found along the fiber. Therefore, the new limit to probe wave power is the effective Brillouin threshold of the sensing fiber. Nevertheless, the probe FM modulation technique that we deploy pushes this limit to higher powers than in standard BOTDA setups. Using our BOTDA setup, we deployed a probe wave of 15 dBm, which, to the best of our knowledge is the largest probe power ever injected in a long-range BOTDA setup. The enhancement in the detected SNR brought by the use of such power leads to an excellent sensor performance without resorting to additional means such as the use of pump pulse coding or Raman gain.

References

[1] X. Angulo-Vinuesa *et al.*, "Raman-assisted brillouin distributed temperature sensor over 100 km featuring 2 m resolution and 1.2 °C uncertainty," *J. Lightwave Technol.*, vol. 30, no. 8, pp. 1060–1065, 2012.
[2] J. J. Mompó, J. Urricelqui, and A. Loayssa, "Brillouin optical time-domain analysis sensor with pump pulse amplification," *Opt. Exp.*, vol. 24, no. 12, pp. 12672–12681, 2016.
[3] L. Thévenaz, S. Mafang, and J. Lin, "Effect of pulse depletion in a Brillouin optical time-domain analysis system," *Opt. Exp.*, vol. 21, no. 12, pp. 14017–14035, 2013.
[4] A. Minardo, R. Bernini, and L. Zeni, "A simple technique for reducing pump depletion in long range distributed Brillouin fiber sensors," *IEEE Sensors J.*, vol. 9, no. 6, pp. 633–634, 2009.
[5] A. Domínguez-López, X. Angulo-Vinuesa, A. López-Gil, S. Martín-López, and M. González-Herráez, "Non-local effects in dual-probe side-band Brillouin optical time domain analysis," *Opt. Exp.*, no. 23, vol. 8, p. 10341, 2015.

[6] A. Domínguez-López *et al.*, "Novel scanning method for distortion-free BOTDA measurements," *Opt. Exp.*, vol. 24, no. 10, pp. 10188–10204, 2016.
[7] X. Hong, W. Lin, Z. Yang, S. Wang, and J. Wu, "Brillouin optical time-domain analyzer based on orthogonally-polarized four-tone probe wave," *Opt. Exp.*, vol. 24, no. 18, pp. 21046–21058, 2016.
[8] R. Ruiz-Lombera, J. Urricelqui, M. Sagues, J. Mirapeix, J. M. López-Higuera, and A. Loayssa, "Overcoming non-local effects and brillouin threshold limitation in brillouin optical time-domain sensors," *IEEE Photon. J.*, vol. 7, no. 6, pp. 1–9, 2015.
[9] G. Agrawal, "Stimulated Brillouin Scattering" in *Proc. Nonlinear Fiber Optics* (Academic, 2013), pp. 358–359.
[10] A. Loayssa, R. Hernández, D. Benito, and S. Galech, "Characterization of stimulated Brillouin scattering spectra by use of optical single-sideband modulation," *Opt. Lett.*, vol. 29, no. 6, pp. 638–640, 2004.
[11] G. H. Smith, D. Novak, and Z. Ahmed, "Technique for optical SSB generation to overcome dispersion penalties in fibre-radio systems," *Electron. Lett.*, vol. 33, no. 1, pp. 74–75, 1997.
[12] M. A. Soto and L. Thévenaz, "Modelling and evaluating the performance of brillouin distributed optical fiber sensors," *Opt. Exp.*, vol. 21, no. 25, pp. 31347–31366, 2013.